Proceedings of the CAS–CERN Accelerator School: Free Electron Lasers and Energy Recovery Linacs, Hamburg, Germany, 31 May–10 June 2016, edited by R. Bailey, CERN Yellow Reports: School Proceedings, Vol. 1/2018, CERN-2018-001-SP (CERN, Geneva, 2018)

High-Gain Regime: 1D[1]

K.-J. Kim[1], *L. Ryan*[2] *and Z. Huang*[3]
[1]The University of Chicago, Illinois, USA
[2]Argonne National Lab, Illinois, USA
[3]Stanford University, California, USA

Abstract
We discuss the free-electron laser physics in high-gain regime in 1D regime, which contains the most important aspects of the free-electron laser dynamics. The high-gain regime is particularly important when mirrors are not available to build oscillators, and has been used as the most straightforward way to produce intense X-rays from FELs.

Keywords
High-gain regime; FELs.

1. Introduction

A free-electron laser (FEL) can act as a high-gain amplifier, in which case the energy exchange during a single pass through the undulator is large and the field amplitude cannot be regarded as a constant. Therefore, it is necessary to consider the field evolution, so that we must study the pendulum equations for the electron motion and Maxwell equation for the radiation. We will derive these equations, limit them to 1D case. An approximate solution of the coupled Maxwell-pendulum equations are obtained to exhibit the basic characteristics.

1 Maxwell equation

An FEL is a natural extension of spontaneous undulator radiation once we include the self-consistent electron motion in the radiation field. Thus we may begin our FEL derivation starting from the paraxial approximation of Maxwell equation [1] for N_e electrons arbitrarily distributed:

$$\left[\frac{\partial}{\partial z} + \frac{\mathrm{i}k}{2}\boldsymbol{\phi}^2\right]\tilde{\mathcal{E}}_\omega(\boldsymbol{\phi};z) = \sum_{j=1}^{N_\mathrm{e}} \frac{e\left[\boldsymbol{\beta}_j(z) - \boldsymbol{\phi}\right]}{4\pi\epsilon_0 c\lambda^2}\mathrm{e}^{\mathrm{i}k[ct_j(z)-z]} \times \int \mathrm{d}x\, \mathrm{e}^{-\mathrm{i}k\boldsymbol{\phi}\cdot\boldsymbol{x}}\delta\left(\boldsymbol{x} - \boldsymbol{x}_j\right). \tag{1}$$

Here, we have rewritten the angular dependence of the current so that we can replace the point-like electron source with a constant charge density in the transverse plane by making the replacement $\delta(\boldsymbol{x} - \boldsymbol{x}_j) \to \mathcal{A}_\mathrm{tr}^{-1}$, where $\mathcal{A}_\mathrm{tr}$ is the transverse area. Then, in the one-dimensional (1D) limit we have

$$\int \mathrm{d}\boldsymbol{x}\, \mathrm{e}^{-\mathrm{i}k\boldsymbol{\phi}\cdot\boldsymbol{x}}\delta\left(\boldsymbol{x} - \boldsymbol{x}_j\right) \to \frac{1}{\mathcal{A}_\mathrm{tr}}\int \mathrm{d}\boldsymbol{x}\mathrm{e}^{-\mathrm{i}k\boldsymbol{\phi}\cdot\boldsymbol{x}} = \frac{\lambda^2}{\mathcal{A}_\mathrm{tr}}\delta(\boldsymbol{\phi}), \tag{2}$$

and the source is directed entirely in the forward direction. We complete the 1D limit by defining the 1D electric field $\tilde{E}_\omega(z)$ via

[1] from Kwang-Je Kim, Zhirong Huang, Ryan Lindberg, Synchrotron Radiation and Free-Electron Lasers (2017), © Cambridge University Press 2017, reproduced with permission. This material cannot be reproduced, shared, altered, or exploited commercially in any way without the permission of Cambridge University Press, as it is copyrighted material and therefore not subject to the allowances permitted by a CC licence.

$$\tilde{\mathcal{E}}_\omega(\boldsymbol{\phi};z) = \tilde{E}_\omega(z)\delta(\boldsymbol{\phi}). \tag{3}$$

The $\delta(\boldsymbol{\phi})$ enforces the field to be in the forward direction only, which also implies that the spatial representation of the electric field is independent of $\boldsymbol{x}$. We insert the field Eq. (3) and the transverse electron velocity $\beta_{x,j} = (K/\gamma_j)\cos(k_u z)$ into Eq. (1), and then integrate over angles to find the 1D field equation

$$\frac{\partial}{\partial z}\tilde{E}_\upsilon(z) = \frac{1}{2\pi}\sum_{j=1}^{N_\mathrm{e}}\frac{eK\cos(k_u z)}{4\epsilon_0 c\mathcal{A}_\mathrm{tr}\gamma_j}\mathrm{e}^{\mathrm{i}k[ct_j(z)-z]}\,. \tag{4}$$

Here $\nu = \frac{\omega}{\omega_1} = \frac{k}{k_1}$ is the dimensionless frequency. We have assumed that the field $\tilde{E}_\nu(z)$ describes a slowly varying envelope, so that consistency requires that we also identify the slowly varying current in Eq. (4). As discussed previously, we can do this by introducing the average particle time $\bar{t}_j = t_j - (K^2/8k_u\gamma^2)\sin(2k_u z)$ that subtracts off the oscillatory figure-eight component from t. In terms of the slowly varying ponderomotive phase, we have

$$\begin{aligned} k[ct_j(z) - z] &= \nu[\omega_1\bar{t}_j(z) - (k_1 + k_u)z] + \nu k_u z + \frac{\nu K^2}{4+2K^2}\sin(2k_u z) \\ &= -\nu\theta_j(z) + \Delta\nu k_u z + hk_u z + \nu\xi\sin(2k_u z)\,, \end{aligned} \tag{5}$$

where we recall that h is an odd integer identifying the harmonic number, the normalized frequency difference $\Delta\nu \equiv \nu - h \equiv k/k_1 - h$, and we have introduced the shorthand notation $\xi \equiv K^2/(4+2K^2)$. Then, the wave equation Eq. (4) becomes

$$\begin{aligned} \frac{\partial}{\partial z}\tilde{E}_\nu(z) = -\frac{eK}{4\epsilon_0 c\mathcal{A}_\mathrm{tr}}\frac{1}{2\pi}\sum_{j=1}^{N_\mathrm{e}}\frac{1}{\gamma_j}\mathrm{e}^{-\mathrm{i}\nu\theta_j(z)+\mathrm{i}\Delta\nu k_u z} \\ \times\left[\mathrm{e}^{\mathrm{i}(h-1)k_u z} + \mathrm{e}^{\mathrm{i}(h+1)k_u z}\right]\mathrm{e}^{\mathrm{i}\nu\xi\sin(2k_u z)}\,. \end{aligned} \tag{6}$$

The envelope $\tilde{E}_\nu(z)$, energy γ_j, and phase $\theta_j(z)$ all vary slowly over one undulator period, as does $\mathrm{e}^{\mathrm{i}\Delta\nu k_u z}$ if we restrict our attention to small frequency detunings, $|\Delta\nu| \ll 1$. We can extract the slowly varying terms from the second line of Eq. (6) by averaging over an undulator period λ_u as follows:

$$\begin{aligned} \frac{1}{\lambda_u}\int_0^{\lambda_u} \mathrm{d}z\left[\mathrm{e}^{\mathrm{i}(h-1)k_u z} + \mathrm{e}^{\mathrm{i}(h+1)k_u z}\right]\mathrm{e}^{\mathrm{i}\nu\xi\sin(2k_u z)} \\ = J_{-(h-1)/2}(\nu\xi) + J_{-(h+1)/2}(\nu\xi) \equiv [\mathrm{JJ}]_h\,, \end{aligned} \tag{7}$$

where we have used the Jacobi–Anger identity to evaluate the integral, from which we find the harmonic Bessel function factor $[\mathrm{JJ}]_h$.

We are now in a position to write the frequency domain wave equation for the 1D FEL. However, there are a few notational issues that we would like to simplify. First, we will find it convenient to have the temporal and frequency representations of the field be related by a Fourier transform with respect to the scaled frequency ν. To do this, we write

$$\begin{aligned} E_x(\boldsymbol{x},t;z) &= \int \mathrm{d}\omega\mathrm{d}\boldsymbol{\phi}\,\mathrm{e}^{-\mathrm{i}(\omega-k\boldsymbol{\phi}\cdot\boldsymbol{x})}\mathrm{e}^{\mathrm{i}kz}\tilde{\mathcal{E}}_\omega(\boldsymbol{\phi};z) = \int \mathrm{d}\omega\,\mathrm{e}^{-\mathrm{i}(\omega-kz)}\tilde{E}_\omega(z) \\ &= \mathrm{e}^{-\mathrm{i}h(\omega_1-k_1 z)}\int \mathrm{d}\nu\;\mathrm{e}^{\mathrm{i}\Delta\nu\theta}ck_1\mathrm{e}^{-\mathrm{i}\Delta\nu k_u z}\tilde{E}_\omega(\mathrm{z})\,. \end{aligned} \tag{8}$$

The integrand contains the slowly varying field, and we can both simplify this and eliminate the phase $\mathrm{e}^{\mathrm{i}\Delta\nu k_u z}$ from the source current in Eq. (6) by defining the phase-shifted electric field amplitude

$$E_\nu(z) = ck_1 \mathrm{e}^{\mathrm{i}\Delta\nu k_u z}\tilde{E}_\omega(z)\,. \tag{9}$$

Note that this phase shift must be retained even though $\Delta\nu \ll 1$, since we may also have $k_u z \gg 1$. Finally, the field equation for $E_\nu(z)$ is

$$\begin{aligned}\left[\frac{\partial}{\partial z} + \mathrm{i}\Delta k_u\right]E_\nu(z) &= \frac{ek_1K[\mathrm{JJ}]_h}{4\epsilon_0\gamma_r\mathcal{A}_{\mathrm{tr}}}\frac{1}{2\pi}\sum_{j=1}^{N_\mathrm{e}}\mathrm{e}^{-\mathrm{i}\nu\theta_j(z)}\\ &= -\kappa_h n_e\frac{1}{N_\lambda}\sum_{j=1}^{N_\mathrm{e}}\mathrm{e}^{-\mathrm{i}\nu\theta_j(z)}\,.\end{aligned} \tag{10}$$

Here, N_λ is the number of electrons in one wavelength, and the harmonic coupling and electron volume density are, respectively,

$$\kappa_h \equiv \frac{eK[\mathrm{JJ}]_h}{4\epsilon_0\gamma_r}, \qquad\qquad n_e \equiv \frac{I/ec}{\mathcal{A}_{\mathrm{tr}}} \equiv \frac{N_\lambda}{\lambda_1\mathcal{A}_{\mathrm{tr}}}\,. \tag{11}$$

Note that while approximating γ_j by γ_r in k_h is a very good approximation, such a replacement in the particle phase would eliminate the FEL interaction entirely.

Equation (10) is in frequency domain, and is the most convenient to analytically study the FEL dynamics [1]. There are situations in which the time domain approach is more useful. The time domain equations are also well-suited for efficient numerical simulation codes. In the rest of this paper we will use the time domain formulation to obtain some basic understanding of the high-gain behaviour and its scalings.

The time domain wave equation basically follows from the inverse Fourier transform of Eq. (10). To make this connection explicit, we use the definitions Eq. (8) and Eq. (9) to find that 1D slowly varying envelopes are related by the Fourier transforms

$$E(\theta;z) = \int \mathrm{d}\nu\, \mathrm{e}^{\mathrm{i}\Delta\nu\theta}E_\nu(z)\,, \qquad\qquad E_\nu(z) = \frac{1}{2\pi}\int \mathrm{d}\theta\, \mathrm{e}^{-\mathrm{i}\Delta\nu\theta}E(\theta;z)\,. \tag{12}$$

Therefore, multiplying Eq. (10) by $\mathrm{e}^{\mathrm{i}\Delta\nu\theta}$ and integrating over ν yields

$$\left[\frac{\partial}{\partial z} + k_u\frac{\partial}{\partial\theta}\right]E(\theta;z) = -\kappa_1 n_e\frac{2\pi}{N_\lambda}\sum_{j=1}^{N_e}\mathrm{e}^{-\mathrm{i}\theta_j(z)}\delta\left[\theta - \theta_j(z)\right]\,, \tag{13}$$

at the fundamental frequency ω_1.

It may appear that our work is done, but the transverse current in Eq. (13) is composed of a sum of delta functions that is unfortunately both difficult to treat and apparently in violation of our assumption that E varies slowly. To establish a well-defined, slowly varying current, we average Eq. (13) over some number of periods in θ. This 'slice-averaging' has the same physical significance as our previous assumption that $|\Delta\nu| \ll 1$, and is valid provided the averaging time is much shorter than the characteristic time over which the field amplitude changes. For a high-gain FEL we require the averaging time Δt to be much less than the coherence time, $\Delta t = \Delta\theta/\omega_h \ll t_{\mathrm{coh}}$, which at the fundamental frequency reduces to $\Delta t \ll \lambda_1/(4\pi c\rho)$ or $\Delta\theta \ll 1/2\rho$. The time window over which the beam average is taken is sometimes referred to as an FEL slice.

We average Eq. (13) over an FEL slice by applying

$$\frac{1}{\Delta\theta}\int_{\theta-\Delta\theta/2}^{\theta+\Delta\theta/2} \mathrm{d}\theta'\Bigg|_{\text{at fixed } z} \tag{14}$$

to both sides. Averaging the left-hand side of Eq. (13) leaves it unchanged since it is slowly varying, while applying Eq. (14) to the right-hand side picks out those electrons whose ponderomotive phase θ_j is within the interval $\theta - \Delta\theta/2$ and $\theta + \Delta\theta/2$. In other words, the source for $E(\theta)$ includes the $N_\Delta = N_\lambda(\Delta\theta/2\pi)$ electrons that satisfy $\left|\theta_j - \theta\right| \leq \Delta\theta/2$ when they arrive at location z. Then, we find that the wave equation in the time domain is

$$\left[\frac{\partial}{\partial z} + k_u\frac{\partial}{\partial\theta}\right]E(\theta;z) = -\kappa_1 n_e \frac{1}{N_\Delta}\sum_{j\epsilon\Delta} \mathrm{e}^{-\mathrm{i}\theta_j(z)} \tag{15}$$

$$= -\kappa_1 n_e \langle \mathrm{e}^{-\mathrm{i}\theta_j(z)}\rangle_\Delta\,. \tag{16}$$

The notation in Eq. (15) denotes that we are to sum over the N_Δ particles within the FEL slice at position z and phase θ. Hence, the average $\langle \mathrm{e}^{-\mathrm{i}\theta_j}\rangle_\Delta$, which is often referred to as the local bunching factor (or just bunching factor), is a function of both z and θ. For any given z, the bunching factor quantifies the spectral content of the current near the fundamental frequency by a complex number whose magnitude is between 0 and 1[2]. Finally, we note while that the Maxwell equation in the time and frequency domain look quite similar, they differ as follows: the driving current in Fourier version Eq. (10) is a sum over all electrons with the phase $\mathrm{e}^{-\mathrm{i}\nu\theta_j}$, while the time domain Eq. (15) sums only over those electrons within the FEL time slice using the phase $\mathrm{e}^{-\mathrm{i}\theta}$.

2 FEL equations and energy conservation

All equations governing the 1D FEL in the time domain are as follows:

$$\left[\frac{\partial}{\partial z} + k_u\frac{\partial}{\partial\theta}\right]E(\theta;z) = -\kappa_1 n_e \langle \mathrm{e}^{-\mathrm{i}\theta_j}\rangle_\Delta\,, \tag{17}$$

$$\frac{\mathrm{d}\theta_j}{\mathrm{d}z} = 2k_u\eta_j\,, \tag{18}$$

$$\frac{\mathrm{d}\eta_j}{\mathrm{d}z} = \chi_1\left(E\mathrm{e}^{\mathrm{i}\theta_j} + E^*\mathrm{e}^{-\mathrm{i}\theta_j}\right), \tag{19}$$

with

$$\kappa_1 \equiv \frac{\mathrm{e}K[\mathrm{JJ}]}{4\epsilon_0\gamma_r}\,, \qquad \chi_1 \equiv \frac{\mathrm{e}K[\mathrm{JJ}]}{2\gamma_r^2 mc^2}\,. \tag{20}$$

Equations (17) is Maxwell equation (the same as Eq. (16)) and Eqs. (18) and (19) are the pendulum equations describing the electron motion [1]. These equations conserve total (particle + field) energy. To show this, we first integrate the electromagnetic energy density u_{EM} over length and multiply the result by the transverse area $\mathcal{A}_{\mathrm{tr}}$ to obtain the field energy

$$U_{\mathrm{EM}} = \frac{\mathcal{A}_{\mathrm{tr}}\lambda_1}{2\pi}\int \mathrm{d}\theta\; u_{\mathrm{EM}} = \frac{\mathcal{A}_{\mathrm{tr}}\lambda_1}{2\pi}\int \mathrm{d}\theta\,\frac{\epsilon_0}{2}\left(\boldsymbol{E}^2 + c^2\boldsymbol{B}^2\right)$$

[2] Harmonic generalizations of the bunching factor can also be defined as $b_h \equiv \langle \mathrm{e}^{-\mathrm{i}h\theta_j}\rangle_\Delta$.

$$= \frac{\mathcal{A}_{\text{tr}}\lambda_1}{2\pi} \int \mathrm{d}\theta \; 2\epsilon_0 |E|^2 \,. \tag{21}$$

Hence, an equation for the electromagnetic field energy can be obtained by multiplying (Eq. (17)) by $(\mathcal{A}_{\text{tr}}\lambda_1/\pi)\epsilon_0 E^*$, adding the complex conjugate, and integrating over θ; we find that

$$\begin{aligned}
\frac{\mathrm{d}}{\mathrm{d}z} U_{\text{EM}} &= -\frac{\mathrm{e}K[\text{JJ}]}{2\gamma_r} \frac{N_\lambda}{2\pi N_\Delta} \int \mathrm{d}\theta \sum_{j\epsilon\Delta} E^* \mathrm{e}^{-\mathrm{i}\theta j} + c.c. \\
&= -\frac{\mathrm{e}K[\text{JJ}]}{2\gamma_r} \sum_j \frac{\mathrm{e}^{-\mathrm{i}\theta_j}}{\Delta\theta} \int_{\theta_j-\Delta\theta/2}^{\theta_j+\Delta\theta/2} \mathrm{d}\theta \; E^*(\theta) + c.c. \\
&= -\frac{\mathrm{e}K[\text{JJ}]}{2\gamma_r} \sum_j E^*(\theta_j) \mathrm{e}^{-\mathrm{i}\theta_j} + c.c.\,,
\end{aligned} \tag{22}$$

where in the last line we assumed that $E(\theta)$ is constant over the length $\Delta\theta$; this assumption is required because of our slice averaging, but is not necessary if one uses the frequency representation (Eq. (10)) or the unaveraged Eq. (13). The change in the total kinetic energy is obtained by multiplying (Eq. (19)) by $\gamma_r mc^2$ and summing over all electrons,

$$\frac{\mathrm{d}}{\mathrm{d}z} U_{\text{KE}} = \frac{\mathrm{d}}{\mathrm{d}z} \sum_j \gamma_r (1 + \eta_j) mc^2 = \frac{\mathrm{e}K[\text{JJ}]}{2\gamma_r} \sum_j E(\theta_j) \mathrm{e}^{\mathrm{i}\theta_j} + c.c. \tag{23}$$

Adding Eqs. (22) and (23) shows that energy is conserved:

$$\frac{\mathrm{d}}{\mathrm{d}z} [U_{\text{EM}} + U_{\text{EM}}] = \frac{\mathrm{d}}{\mathrm{d}z} \left[\sum_j \gamma_r n_j mc^2 + \frac{\mathcal{A}_{\text{tr}}\lambda_1}{2\pi} \int \mathrm{d}\theta \; 2\epsilon_0 |E(\theta; z)|^2 \right] = 0\,. \tag{24}$$

3 Dimensionless FEL scaling parameter ρ

By expressing the governing equations of physical systems in terms of dimensionless quantities, one can identify important time and length scales and characterize the relevant magnitudes of the physical variables. In this section we cast the FEL equations into dimensionless form and find the fundamental scaling parameter ρ. We will subsequently see that ρ, which is also called the Pierce parameter, characterizes most properties of a high-gain FEL, while the dimensionless beam and radiation variables will give us some sense of the dynamics without any additional computation.

We introduce the as-yet-unspecified parameter ρ by defining the scaled longitudinal coordinate $\hat{z} \equiv 2k_u\rho z$ that leads to the phase equation

$$\frac{\mathrm{d}\theta_j}{\mathrm{d}\hat{z}} = \hat{\eta}_j \text{ for } \hat{\eta}_j \equiv \frac{\eta_j}{\rho} \qquad \text{(the new 'momentum' variable).} \tag{25}$$

To simplify the energy equation for $\hat{\eta}_j$, we define the dimensionless complex field amplitude

$$a = \frac{\chi_1}{2k_u\rho^2} E\,, \tag{26}$$

in terms of which the energy equation reduces to

$$\frac{\mathrm{d}\hat{\eta}_j}{\mathrm{d}\hat{z}} = a(\theta_j, \hat{z}) \mathrm{e}^{\mathrm{i}\theta_j} + a(\theta_j, \hat{z})^* \mathrm{e}^{-\mathrm{i}\theta_j}\,. \tag{27}$$

Writing the field Eq. (17) in terms of $\hat{z}$ and a, we have

$$\left[\frac{\partial}{\partial \hat{z}} + \frac{1}{2\rho}\frac{\partial}{\partial \theta}\right] a(\theta, \hat{z}) = -\frac{\chi_1}{2k_u\rho^2}\frac{n_e\kappa_1}{2k_u\rho}\langle \mathrm{e}^{-\mathrm{i}\theta_j}\rangle_\Delta \,. \tag{28}$$

To simplify the field equation, we choose to set the coefficient on the right-hand side of Eq. (28) to unity. Thus, the dimensionless Pierce parameter ρ must be [1]

$$\rho = \left[\frac{n_e\kappa_1\chi_1}{(2k_u)^2}\right]^{1/3} = \left(\frac{e^2K^2[\mathrm{JJ}]^2 n_e}{32\epsilon_0\gamma_r^3 mc^2 k_u^2}\right)^{1/3}$$

$$= \left[\frac{1}{8\pi}\frac{I}{I_\mathrm{A}}\left(\frac{K[\mathrm{JJ}]}{1+K^2/2}\right)^2 \frac{\gamma\lambda_1^2}{2\pi\sigma_x^2}\right]^{\frac{1}{3}} , \tag{29}$$

where $I_\mathrm{A} = ec/r_e = 4\pi\epsilon_0 mc^3/e \approx 17045$ A is the Alfvén current and we have set the cross-sectional area of the electron beam $\mathcal{A}_\mathrm{tr} \to 2\pi\sigma_x^2$ assuming a Gaussian transverse profile.

The scaled FEL equations have all coefficients unity, so that the dimensionless form allows one to make a number of order-of-magnitude estimates regarding the dynamics. First, one may *a priori* expect that the scaled variation $\mathrm{d}/\mathrm{d}\hat{z} \lesssim 1$. Thus, in the exponential growth regime we may anticipate the 1D gain length $L_{G0} \sim (2k_u\rho)^{-1}$. Additionally, since resonant energy exchange proceeds if the ponderomotive phase is nearly constant, this implies that saturation of the FEL interaction occurs when the scaled energy deviation $\hat{\eta}_j \sim 1$ (or $\eta_j \sim \rho$). At this point we expect that the bunching will approach its maximum value $\left|\langle \mathrm{e}^{-\mathrm{i}\theta_j}\rangle_\Delta\right| \to 1$, which in turn implies that the maximum scaled amplitude of the radiation $|a| \sim 1$. Furthermore, if we had included the transverse derivatives in the wave equation we would expect

$$\frac{1}{4k_u k_1 \rho}\boldsymbol{\nabla}_\perp^2 \to 1 \,. \tag{30}$$

Identifying the transverse Laplacian with the radiation size via $\boldsymbol{\nabla}_\perp^2 \sim 1/\sigma_r^2$ we find that the RMS mode size of the laser is roughly given by

$$\sigma_r \sim \sqrt{\frac{\lambda_1}{4\pi}\frac{\lambda_u}{4\pi\rho}} \,. \tag{31}$$

While these arguments are heuristic, they give useful predictions of FEL performance. Besides the observation that the gain length is approximately $\lambda_u/4\pi\rho$, we use the definition Eq. (26) to translate the scaled radiation amplitude $|a| \to 1$ at saturation to $|E| \to 2k_u\rho^2/\chi_1$, so that the maximum field energy density

$$2\epsilon_0|E|^2 \sim 2\epsilon_0\rho\frac{4k_u\rho^3}{\chi_1^2} = 2\epsilon_0\rho\frac{\kappa_1}{\chi_1} = \rho n_e\gamma_r mc^2 \,. \tag{32}$$

Because $n_e mc^2\gamma_r$ is the electron energy density, we see that ρ also gives the FEL efficiency at saturation:

$$\rho = \frac{\text{field energy generated}}{\text{e-beam kinetic energy}} \,. \tag{33}$$

To determine the distance at which the FEL gain saturates and $P \sim \rho P_\mathrm{beam}$, we consider the motion of the electron in the pendulum potential. The period of motion is characterized by the synchrotron wavenumber

$$\Omega_s \equiv \sqrt{\frac{eE_0k_uK[\mathrm{JJ}]}{\gamma^2mc^2}} = 2\rho k_u|2a_0|^{1/2} , \tag{34}$$

and that the radiation field gains or loses energy depending on the oscillation phase of the particles. Since the energy exchange to the radiation ends when most of the particles make one-half oscillation in the ponderomotive bucket, we have $\langle\Omega_s\rangle z_{\text{sat}} \approx \pi$, where $\langle\Omega_s\rangle$ is the average value of the synchrotron wavenumber over the FEL length z_{sat}. Taking $\langle\Omega_s\rangle$ to be one-quarter of its maximum value at saturation where $|a_0| \sim 1$, we have $\rho k_u z_{\text{sat}}/\sqrt{2} \sim \pi$, or $z_{\text{sat}} \sim \lambda_u/\rho$. It is interesting to note that the power saturates when the synchrotron wavenumber is roughly equal to the exponential growth rate,

$$P \sim \rho P_{\text{beam}} \Leftrightarrow \Omega_s \sim 2\rho k_u . \tag{35}$$

This is to be expected, since when $\Omega_s \sim 2\rho k_u$ the particles can rotate to the accelerating phase of the potential during one growth length, in which case they then extract energy from the field.

Therefore, the FEL (or Pierce) parameter ρ determines the main characteristics of high-gain FEL systems, including the following.

1. Gain length $\sim \lambda_u/4\pi\rho$.
2. Saturation power $\sim \rho\times$ (e-beam power).
3. Saturation length $_{\text{sat}} \sim \lambda_u/\rho$.
4. Transverse mode size $\sigma_r \sim \sqrt{\lambda_1\lambda_u/16\pi^2\rho}$.

In the following sections we will analyse the FEL equations and demonstrate that the dynamics indeed exhibit these simple scalings.

4 1D solution using collective variables

In this section, we illustrate the essentials of FEL gain by neglecting the θ dependence of the electromagnetic field. This ignores the propagation (slippage) of the radiation, and is equivalent to assuming that a has only one frequency component. This model will be useful to illustrate the basic physics of the electron beam and radiation field in a high-gain device, but will be insufficient to fully understand the spectral properties of self-amplified spontaneous emission (SASE). A more rigorous discussion of SASE can be found in literature [1]. The 1D FEL equations ignoring radiation slippage are as follows

$$\frac{\mathrm{d}\theta_j}{\mathrm{d}\hat{z}} = \hat{\eta}_j, \tag{36}$$

$$\frac{\mathrm{d}\hat{\eta}_j}{\mathrm{d}\hat{z}} = a\mathrm{e}^{\mathrm{i}\theta_j} + a^*\mathrm{e}^{-\mathrm{i}\theta_j}, \tag{37}$$

$$\frac{\mathrm{d}a}{\mathrm{d}\hat{z}} = -\langle \mathrm{e}^{-\mathrm{i}\theta_j}\rangle_\Delta . \tag{38}$$

These are $2N_\Delta + 2$ coupled first-order ordinary differential equations, $2N_\Delta$ for the particles, and 2 for the complex amplitude a. In general, these can only be solved via computer simulation. However, the system can be linearized in terms of three collective variables as in Ref. [2]:

$$\begin{aligned} &a && \text{(field amplitude);}\\ &b = \langle \mathrm{e}^{-\mathrm{i}\theta_j}\rangle_\Delta && \text{(bunching factor);}\\ &P = \langle \hat{\eta}_j \mathrm{e}^{-\mathrm{i}\theta_j}\rangle_\Delta && \text{(collective momentum) .} \end{aligned}$$

The equations of motion for the bunching b and the field amplitude a follow directly from Eqs. (36) and (38). Differentiating the collective momentum yields

$$\frac{\mathrm{d}P}{\mathrm{d}\hat{z}} = \left\langle \frac{\mathrm{d}\hat{\eta}_j}{\mathrm{d}\hat{z}} \mathrm{e}^{-\mathrm{i}\theta_j} \right\rangle - \mathrm{i}\langle \hat{\eta}_j^2 \mathrm{e}^{-\mathrm{i}\theta_j} \rangle = a + a^* \langle \mathrm{e}^{-2\mathrm{i}\theta_j} \rangle - \mathrm{i}\langle \hat{\eta}_j^2 \mathrm{e}^{-\mathrm{i}\theta_j} \rangle . \quad (39)$$

Note that Eq. (39) contains additional field variables, and the resulting system of equations is not closed. Nevertheless, these other terms are nonlinear, which we therefore expect to result in negligible higher-order corrections when a, b, and P are much smaller than unity before saturation. Thus, linearizing Eq. (39) and including the equations for b and a from Eqs. (36) and (38) yields the following closed system in the small-signal regime:

$$\frac{\mathrm{d}a}{\mathrm{d}\hat{z}} = -b \qquad \text{bunching produces coherent radiation} , \quad (40a)$$

$$\frac{\mathrm{d}b}{\mathrm{d}\hat{z}} = -\mathrm{i}P \qquad \text{energy modulation becomes density bunching}, \quad (40b)$$

$$\frac{\mathrm{d}P}{\mathrm{d}\hat{z}} = a \qquad \text{coherent radiation drives energy modulation} . \quad (40c)$$

These are three coupled first-order equations, which can be reduced to a single third- order equation for a as

$$\frac{\mathrm{d}^3 a}{\mathrm{d}\hat{z}^3} = \mathrm{i}a . \quad (41)$$

We solve the linear equation by assuming that the field dependence is $\sim \mathrm{e}^{-\mathrm{i}\mu\hat{z}}$, which results in the following dispersion relation for μ:

$$\mu^3 = 1 . \quad (42)$$

This is the well-known cubic equation, whose three roots are given by

$$\mu_1 = 1 , \qquad \mu_2 = \frac{-1 - \sqrt{3}\mathrm{i}}{2} , \qquad \mu_3 = \frac{-1 + \sqrt{3}\mathrm{i}}{2} . \quad (43)$$

The root μ_1 is real and gives rise to an oscillatory solution, while μ_2 and μ_3 are complex conjugates that lead to exponentially decaying and growing modes, respectively. Furthermore, the roots obey

$$\sum_{\ell=1}^{3} \mu_\ell = 0, \qquad \sum_{\ell=1}^{3} \frac{1}{\mu_\ell} = \sum_{\ell=1}^{3} \mu_\ell^* = \sum_{\ell=1}^{3} \mu_\ell^2 = 0 , \quad (44)$$

and the general solution to Eq. (41) is composed of a linear combination of the exponential solutions:

$$a(\hat{z}) = \sum_{\ell=1}^{3} C_\ell \mathrm{e}^{-\mathrm{i}\mu_\ell \hat{z}} . \quad (45)$$

The three constants C_ℓ are determined from the initial conditions $a(0)$, $b(0)$, and $P(0)$. By differentiating the expression for a and using Eq. (40), we find

$$a(0) = C_1 + C_2 + C_3 , \quad (46)$$

$$\left.\frac{\mathrm{d}a}{\mathrm{d}\hat{z}}\right|_0 = -b(0) = -\mathrm{i}[\mu_1 C_1 + \mu_2 C_2 + \mu_3 C_3] , \quad (47)$$

$$\left.\frac{\mathrm{d}^2 a}{\mathrm{d}\hat{z}^2}\right|_0 = iP(0) = -[\mu_1^2 C_1 + \mu_2^2 C_2 + \mu_3^2 C_3] . \quad (48)$$

Using Eq. (44), this yields the electromagnetic field evolution as

$$a(\hat{z}) = \frac{1}{3}\sum_{\ell=1}^{3}\left[a(0) - \mathrm{i}\frac{b(0)}{\mu_\ell} - \mathrm{i}\mu_\ell P(0)\right]\mathrm{e}^{-\mathrm{i}\mu_\ell \hat{z}} \,. \tag{49}$$

The general solution for the radiation requires all three roots of μ. For long propagation distances, however, the relative importance of the oscillating root μ_1 and decaying root μ_2 becomes insignificant in comparison with the growing solution associated with μ_3. Thus, the radiation field is completely characterized by μ_3 in the exponential growth regime where $\hat{z} \gg 1$, so that

$$a(\hat{z}) \approx \frac{1}{3}\left[a(0) - \mathrm{i}\frac{b(0)}{\mu_3} - \mathrm{i}\mu_3 P(0)\right]\mathrm{e}^{-\mathrm{i}\mu_3 \hat{z}} \,. \tag{50}$$

The first term in the bracket describes the coherent amplification of an external radiation signal, while the second and the third term show how modulations in the electron beam density and energy may lead to FEL output. When the source of these modulations is the electron beam shot noise then the exponential growth is considered to be SASE.

5 Qualitative description of SASE

SASE results from the FEL amplification of the initially incoherent spontaneous undulator radiation, Refs. [2, 3, 4]. It is of primary importance for FEL applications in wavelength regions where mirrors (and, hence, oscillator configurations) are unavailable.

For our first look at SASE, we use the formula for the radiation in the high-gain regime Eq. (50) assuming that there is no external field $a(0) = 0$ and that the beam has vanishing energy spread with $P(0) = 0$. In this case, the radiation intensity in the exponential growth regime is

$$\langle |a(\hat{z})|^2\rangle \approx \frac{1}{9}\langle |b(0)|^2\rangle \mathrm{e}^{\sqrt{3}\hat{z}} \,. \tag{51}$$

Here, the scaled propagation distance $\sqrt{3}\hat{z} = \sqrt{3}(2k_u z\rho) = z/L_{G0}$, and the ideal 1D power gain length is

$$L_{G0} \equiv \frac{\lambda_u}{4\pi\sqrt{3}\rho} \,. \tag{52}$$

The bunching factor at the undulator entrance $\langle |b(0)|^2\rangle$ derives from the initial shot noise of the beam, which is subsequently amplified by the FEL process. This level of shot noise is determined by the number of particles in the radiation coherence length, and it can be shown that

$$\langle |b(0)|^2\rangle = \left\langle \frac{1}{N_{l_\mathrm{coh}}^2}\left|\sum_{j\epsilon l_\mathrm{coh}} \mathrm{e}^{-\mathrm{i}\theta_j}\right|^2\right\rangle \approx \frac{1}{N_{l_\mathrm{coh}}} \,, \tag{53}$$

where N_{l_coh} is the number of electrons in a coherence length l_coh. It turns out that the normalized bandwidth of SASE is $\Delta\omega/\omega \sim \rho$, so that the coherence time $t_\mathrm{coh} \sim \lambda_1/c\rho$ and the coherence length $l_\mathrm{coh} \sim \lambda_1/\rho$ [2]. Alternatively, one can recognize the coherence length as the amount the radiation slips ahead of the electron beam in a few gain lengths. Hence, the start-up noise of a SASE FEL is characterized by

$$N_{l_\mathrm{coh}} \sim \frac{I}{ec}\frac{\lambda_1}{\rho} \,. \tag{54}$$

Figure 1 is a schematic plot that illustrates the initial start-up, exponential growth, and saturation of a SASE FEL. As is clear from the figure and from the previous discussion, ρ plays a fundamental role in the high-gain FEL physics for SASE. While we have not yet derived all the radiation properties, some of the important ones include:

1. saturation length $L_{sat} \sim \lambda_u/\rho$;
2. output power $\sim \rho \times P_{\text{beam}}$;
3. frequency bandwidth $\Delta\omega/\omega \sim \rho$;
4. 1D power gain length $L_{G0} = \lambda_u/(4\pi\sqrt{3}\rho)$;
5. transverse coherence: radiation emittance $\varepsilon_r = \lambda/4\pi$;
6. transverse mode size: $\sigma_r \sim \sqrt{\varepsilon_r L_{G0}}$;
7. for the SASE power $P = P_{\text{in}} \exp(z/L_G)$, the effective noise $P_{\text{in}} \sim \rho\gamma mc^2/N_{l_{\text{coh}}}$.

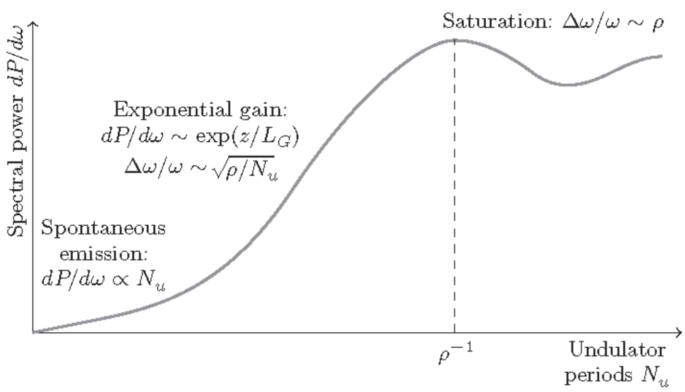

Fig. 1: Illustration of basic SASE processes. Adapted from Ref. [5]

While these basic scalings and the plot of Fig. 1 describes the ensemble averaged SASE properties, we should keep in mind that any individual SASE pulse is essentially amplified undulator radiation, and therefore has the same basic power and spectral fluctuations as the chaotic light discussed in "Temporal Coherence of Radiation Beam from a collection of Electrons" (previous lecture from these proceedings). We can understand the connection of SASE to amplified undulator radiation by considering the undulator energy as computed from the 1D power spectral density,

$$U_{\text{und}} = T\int \mathrm{d}\omega\, \mathrm{d}\boldsymbol{\phi}\, \frac{\mathrm{d}P}{\mathrm{d}\omega\, \mathrm{d}\boldsymbol{\phi}} \xrightarrow{\text{1D}} T\int\, d\omega \frac{\lambda^2}{\mathcal{A}_{\text{tr}}} \frac{\mathrm{d}P}{\mathrm{d}\omega\, \mathrm{d}\boldsymbol{\phi}}\bigg|_{\boldsymbol{\phi}=\mathbf{0}}, \tag{55}$$

where the quantity $\lambda^2/\mathcal{A}_{\text{tr}}$ can be understood as the characteristic angular spread from a source of area $\mathcal{A}_{\text{tr}}$: $\Delta\phi_x\Delta\phi_y \sim \lambda^2/\mathcal{A}_{\text{tr}}$. In the 1D limit this tends to zero and we identify $\delta(\boldsymbol{\phi}) = \mathcal{A}_{\text{tr}}/\lambda^2$, so that

$$\frac{\mathrm{d}P}{\mathrm{d}\omega}\bigg|_{\text{1D}} = \frac{\lambda^2}{\mathcal{A}_{\text{tr}}}\delta(\boldsymbol{\phi})\frac{\mathrm{d}P}{\mathrm{d}\omega} = \frac{\lambda^2}{\mathcal{A}_{\text{tr}}}\frac{\mathrm{d}P}{\mathrm{d}\omega\boldsymbol{\phi}}\bigg|_{\boldsymbol{\phi}=\mathbf{0}}. \tag{56}$$

The same factor $\lambda^2/\mathcal{A}_{\text{tr}}$ appeared for the 1D limit in Eq. (2). Inserting the power density in the forward direction [1], we find that

$$\begin{aligned} U_{\text{und}} &= T\left[\frac{\lambda_1^2}{\mathcal{A}_{\text{tr}}}\frac{I}{I_A}\left(\frac{K[\text{JJ}]}{1+K^2/2}\right)^2 \gamma_r^2 mc^2 N_u^2\right]\frac{\omega_1}{\pi N_u}\int\, \mathrm{d}x\left(\frac{\sin x}{x}\right)^2 \\ &= 8\pi\omega_1 T\gamma_r mc^2 N_u\rho^2 \;\rightarrow 8\pi\omega_1 T\gamma_r mc^2\rho^2 \end{aligned} \tag{57}$$

at the FEL saturation distance $N_u \approx 1/\rho$. Now, we use Eq. (57) to rewrite the FEL energy at saturation as

$$U_{\mathrm{FEL}} = N_{\mathrm{e}}\rho\gamma_r mc^2 = \frac{N_{\mathrm{e}}}{\rho\omega_1 T}\frac{U_{\mathrm{und}}}{8\pi} \sim \frac{t_{\mathrm{coh}}N_{\mathrm{e}}}{T}U_{\mathrm{und}} = N_{l_{\mathrm{coh}}}U_{\mathrm{und}} \tag{58}$$

$$= \frac{T}{t_{\mathrm{coh}}}N_{l_{\mathrm{coh}}}^2\frac{U_{\mathrm{und}}}{N_{\mathrm{e}}}\,. \tag{59}$$

The first line Eq. (58) shows that in the forward direction the FEL output at saturation is larger than that of the undulator radiation by the number of particles in a coherence time $N_{l_{\mathrm{coh}}} \gtrsim 10^5$. The second result Eq. (59) interprets the FEL energy as being proportional to the undulator field energy due to a single electron times the square of the number of electrons in a coherence length times the number of coherent regions T/t_{coh}.

Finally, we would like to emphasize that X-ray FELs based on SASE would not have been realized without incredible improvements in the production, transport, and manipulation of electron beams, since very high brightness electron beams are essential for X-ray FELs. In particular, SASE FELs have been made possible through recent advances in photocathode gun design (see Ref. [6] and a review in Ref. [7]), and tremendous improvements of radiofrequency linac and undulator technology. These advances have made it possible to produce sufficient gain in the undulator for transversely coherent radiation, meaning that the electron beam meets the following criteria:

1. energy spread $\Delta\gamma/\gamma < \rho$;
2. emittance $\varepsilon_x \lesssim \lambda/(4\pi)$;
3. beam size $\sigma_x \gtrsim \sigma_r \sim \sqrt{\frac{\lambda}{4\pi}\frac{\lambda_u}{4\pi\rho}}$ to have 1D scalings approximately apply;
4. high peak current to achieve $\rho \sim 10^{-3}$ and, hence, a reasonable saturation length and power efficiency.

References

[1] See, for example, K.-J. Kim, Z. Huang, and R. Lindberg, "*Synchrotron Radiation and Free-Electron Lasers*," Cambridge University Press (2017).

[2] R. Bonifacio, C. Pellegrini and L.M. Narducci, *Opt. Commun.* **50** (1984) 373. https://doi.org/10.1016/0030-4018(84)90105-6

[3] A. Kondratenko and E. Saldin, *Part. Accel.* **10** (1980) 207.

[4] Y.S. Derbenev, A.M. Kondratenko and E.L. Saldin, *Nucl. Instrum. Methods Phys. Res.* **193** (1982) 415. https://doi.org/10.1016/0029-554x(82)90233-6

[5] K.-J. Kim, *Phys. Rev. Lett.* **57** (1986) 1871. https://doi.org/10.1103/PhysRevLett.57.1871

[6] J.S. Fraser, R.L. Sheffield and E.R. Gray, *Nucl. Instrum. Methods Phys. Res., Sect. A* **250** (1986) 71. https://doi.org/10.1016/0168-9002(86)90862-4

[7] I. Ben-Zvi, in *Accelerator Physics, Technology, and Applications*, Eds. A.W. Chao, H.O. Moser and Z. Zhao (World Scientific, 2004), p. 158. https://doi.org/10.1142/9789812702807_0007